Available online at www.sciencedirect.com
SCIENCE DIRECT®
ELSEVIER
International Journal of Heat and Mass Transfer 47 (2004) 2493–2499
International Journal of HEAT and MASS TRANSFER
www.elsevier.com/locate/ijhmt

Technical Note

Mass transfer from a rotating cylinder with and without crossflow

L. Labraga [a,*], T. Berkah [b]

[a] Laboratoire de Mécanique et d'Energétique, Université de Valenciennes et du Hainaut-Cambrésis, 59313 Valenciennes Cedex 9, France
[b] Department of Mechanical Engineering, Diponegoro University, Semarang, Indonesia

Received 19 March 2003

1. Introduction

The flow around a steady circular cylinder is considered as being of importance to both fundamental and applied thermofluiddynamics. Among the main issues of the classical flow configuration are vortex shedding, boundary layer separation, lift and drag forces, wake patterns and heat or mass transfer. Studies of heat transfer on a smooth steady cylinder have been widely reported in the literature [1,2]. Scholten and Murray [3], carried out simultaneous measurements of the fluctuating heat transfer and velocity using a hot film sensor and a laser Doppler anemometer respectively. They confirmed that the origin of the heat transfer fluctuations in the laminar region in front of the cylinder was a consequence of the vortex shedding behind the cylinder. Heat or mass transfer in flows around a rotating cylinder has rarely been tackled in spite of considerable technological interest. Indeed, any rotating component of various types of machinery can be idealized in terms of a cylinder rotating in crossflow. Kays and Bjorklund [4] measured heat transfer from a rotating cylinder with and without crossflow. They showed that the combined effects of rotation, free convection and crossflow can be correlated by an equation. However, this correlation is limited to rather a low narrow range of Reynolds numbers. Moreover, only global Nusselt numbers are determined, making difficult the instantaneous estimation of the contribution of each region to heat transfer of the rotating cylinder. Peller et al. [5] carried out heat transfer experiments with a heated and rotating cylinder in crossflow. Their experiments took into account some important parameters such as freestream-turbulence intensity, aspect ratio, blockage ratio, and temperature leading. They found that for $\alpha < 0.5$, there are significant deviations from the heat transfer coefficients previously believed to be constant. Peller [6] studied the boundary layer around a heated and rotating cylinder. He showed that increasing the cylinder surface temperature strongly affects the separation separation. Peller and Straub [7] showed that the increase in heat transfer for $\alpha > 2$, is caused by a significant change in the stream moving part of the cylinder. In this case, they concluded that the rotation rate of the cylinder and not the crossflow determines the level of heat transfer. Shimada et al. [8] measured the local and average coefficients of heat transfer from a rotating cylinder with and without crossflow by employing a Mach–Zehnder interferometer associated to a thermal visualization with a high-speed video tape recorder. They found that when $Re_\infty > 1000$ and $\alpha < 1$, the average Nusselt number agreed with the value for the static cylinder in forced convection, and when $Re_\infty < 1000$ and $\alpha > 2$, the heat transfer was poorest. The analogy between heat and mass transfer may be applied to determine heat transfer by measuring mass transfer rates. This technique avoids difficulties associated with accurate measurements of heat transfer coefficients. The mass transfer technique often used, based on naphthalene sublimation is only suitable for steady flows [9]. Moreover, the geometric modification due to sublimation reduces the spatial resolution. Therefore, a suitable method for such measurements is required. The electrochemical technique, allowing the measurement of the local mass transfer in unsteady flow, seems to be appropriate. The present paper reports the results of local mass transfer from a rotating cylinder at various speeds with and without crossflow by using the electrochemical technique. This is an extension of the previous study by Kays and Bjorklund [4]. The local mass transfer results are presented in the form of the variation in phase and time-averaged Sherwood numbers. By analogy, the mass transfer results obtained here, can be transformed into their heat transfer counterparts. The experimental non-intrusive method used in

* Corresponding author. Fax: +32-7511961/33-3275-511-961.
E-mail address: llabraga@univ-valenciennes.fr (L. Labraga).

0017-9310/$ - see front matter
doi:10.1016/j.ijheatmasstransfer.2003.11.008

Nomenclature

A	electrode area
C_0	bulk concentration
C_f	friction coefficient, $2\tau/\rho U_p^2$
d	cylinder diameter
D	diffusivity of the active species
F	Faraday's constant
Gr	Grashof number
I	electrical current
K	mass transfer coefficient
Nu	Nusselt number
Pr	Prandtl number
Sh	Sherwood number, Kd/D
Re_∞	free stream Reynolds number, $U_\infty d/v$
Re_Ω	rotating Reynolds number, $U_p d/v$
Sc	Schmidt number, v/D
S	velocity gradient at the wall
U	streamwise velocity
U_p	peripheral velocity
U_∞	undisturbed streamwise velocity
α	ratio between the peripheral speed of the cylinder and the free stream velocity, U_p/U_∞
θ	angular position measured from the cylinder leading edge
v	kinematic viscosity

this study would provide more detailed understanding of the interaction between momentum and energy transfer in crossflows around rotating circular cylinders.

2. Experimental apparatus and method

The 300×300-mm^2 water channel, the test cylinder for measuring the local wall shear stress and the data acquisition system are described in detail in a previous paper [10]. The present report thus presents only a brief recapitulation. The local mass transfer was determined using the polarographic method. The test fluid was an aqueous solution of potassium iodide [KI] in a concentration of 0.1 mole/l and iodine [I_2] in a concentration of 10^{-3} mole/l. The mass transfer coefficient K, was determined under diffusion controlled conditions on the cathode. The current I flowing to the test electrode of area A is related to the mass transfer coefficient K by

$$K = \frac{I}{A n_e F C_0} \tag{1}$$

where n_e is the number of electrons involved in the reaction.

The mass transfer coefficient K is used to determine the Sherwood number

$$Sh = \frac{Kd}{D} \tag{2}$$

The cylinder had a length of 300 mm and a diameter of 29 mm. The surface of the cylinder for the mass transfer measurements is completely covered with a thin platinum layer. The electrode for the local mass transfer placed in the same position as in the case of the previous wall shear stress measurements, consists of a 1.5 mm diameter platinum probe insulated from the surrounding. Both the isolated cathode and the main cathode were active during the measurements. The data acquisition system includes a mercury slipringless transmitter that performs the coupling of electrical signals from the rotating parts to the non-rotating surroundings. The current from the electrode was at first amplified and converted to a voltage output by an operational amplifier. The output voltage was then digitized and sampled by a Personal Computer. A photocell provided a trigger signal to start data sampling in each period when the cylinder reached a certain position. One hundred and twenty samples per period for each channel were taken in equal time intervals, and a total of more than 1000 periods of data were collected in each experiment. In order to remove random fluctuations from the organized oscillation, the data were phase averaged in the following manner: $\langle K\rangle = \overline{K(t_i)} = \frac{1}{N}\sum_{j=1}^{N} K_j(t_i)$, where j and N represent respectively the record number and the number of records.

The experiments were performed at velocities from 0.25 to 2.5 m/s, and α-values from 0 to 6.92.

2.1. Experimental uncertainties

The diameter of the cylinder and the channel width yield a blockage ratio of 0.1. Therefore, the boundary layer development around the cylinder may be considered as minimally affected. The three-dimensional effects are minimized owing to the relatively large aspect ratio of the cylinder (10.3). Moreover, the electrochemical probe is flush-mounted on the cylinder in the symmetry plane of the test section. The experimental uncertainties associated with the measured Sherwood number (Sh), are mainly due to systematic errors resulting from the estimation of the bulk concentration C_0 and to the effective probe area. The estimated uncertainty of C_0 is less than 2% and that of the probe area is about 7%. Therefore, the experimental uncertainty in the final evaluation of Sh is less than 10%.Another source of error is due to the cylinder position. The angular position of the probe can be located with an error of ±1°.

3. Results

3.1. Mass transfer on a stationary cylinder in crossflow

The mass transfer is illustrated in Fig. 1 in the form of $\frac{Sh}{Sh_0}$, where $Sh_0 = Re_\infty^{1/2} Sc^{1/3}$ and $Sc = 750$, for several Reynolds numbers. For $Re_\infty \leqslant 34\,000$, the mass transfer increases as θ increases from 0° to about 10°, reaching a maximum value and decreasing steeply as the boundary layer thickness rises. An increase in the mass transfer is observed immediately in the wake downstream of the separation point. For $Re_\infty \geqslant 51\,000$, the local mass transfer exhibits a sharp increase from 0° to a maximum value depending on the Reynolds number. This behavior deviates from the square root of Reynolds number correlation. The increase in Sherwood number for $Re_\infty \geqslant 51\,000$ and to a lesser extent for $Re_\infty \leqslant 34\,000$ in the front stagnation point, agrees well with data from the literature. Experimental data of Scholten and Murray [3] obtained by the measurement of the local heat transfer using a hot film sensor for a low freestream turbulence, are plotted in Fig. 1 in the form of $\frac{Nu}{Nu_0}$ where Nu is the Nusselt number, $Nu_0 = Re_\infty^{1/2} Pr^{1/3}$ for $Pr = 0.7$. The heat transfer distributions for $Re_\infty = 21\,580$ and $Re_\infty = 50\,350$ are in good agreement with those of the local mass transfer for $Re_\infty \leqslant 34\,000$, especially in the region from $\theta = 0°$ until the separation point. However, the Nusselt number is lower than the Sherwood number in the wake region for almost the same Reynolds number. This may be attributed to a thick heat transfer convection zone, more sensitive to the recirculation influence and therefore yielding less heat transfer in this region [11], moreover, the positions of the measurements are well characterized in the mass transfer process involving a thin convection layer. At the stagnation point, it can be seen from Fig. 1 that the agreement between $\frac{Nu}{Nu_0}$ and $\frac{Sh}{Sh_0}$ is excellent, and correlated within ±2% at Reynolds numbers as high as 85 000.

3.2. Mass transfer on a rotating cylinder in crossflow

The phase-averaged Sherwood number was determined every three degrees around the cylinder for different Reynolds numbers. Fig. 2 shows the distribution of the local phase-averaged Sherwood number around the rotating cylinder for a free stream Reynolds number of 85 000. A parameter in this representation is α. With increasing α, the mass transfer distribution becomes asymmetric. At very low rotational speed, the local Sherwood number is fairly similar to that of the non-rotating cylinder, consequently, the mass transfer process is controlled mainly by the crossflow. Fig. 2 also

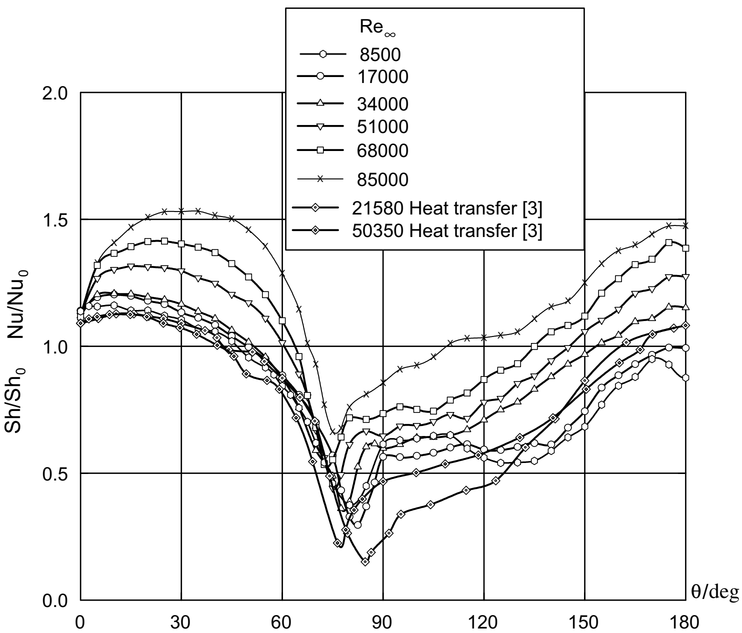

Fig. 1. Local heat and mass transfer around the cylinder ($\alpha = 0$).

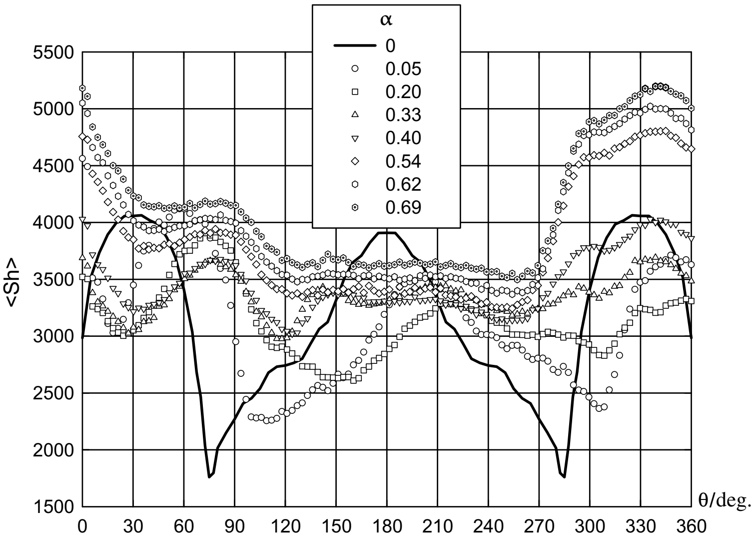

Fig. 2. Phase-averaged mass transfer for $Re_\infty = 85\,000$.

shows that the first minimum value of *Sh*, already observed on the stationary cylinder, still exists on the rotating cylinder. For $\alpha > 0.33$ and for θ between 120° and 270°, mass transfer is at minimum and takes an almost constant value, corresponding to the wake region. This behavior is quite different from that of the non-rotating cylinder, characterized by a large mass transfer at the rear stagnation point, due to the extensive mixing of fluid in the separated flow region. At θ around 180°, the highest *Sh* value is still obtained for the stationary cylinder. The Sherwood number distributions for $Re_\infty = 17\,000$ are plotted in Fig. 3. For this Reynolds number, α increases up to 3.40 generating a quite different behavior of the local mass transfer. The plateau observed on the previous figure disappears. For $\alpha = 3.40$, the Sherwood number distribution tends to that found for mass transfer around a rotating cylinder without crossflow. Kays and Bjorklund [4] found a correlation taking into account effects of combined rotation, crossflow and free convection by plotting Nusselt number as a function of $(0.5Re_\Omega^2 + Re_\infty^2 + Gr)Pr$. For the abscissa from 3×10^7 to 10^9, Their data can be correlated by the equation

$$Nu = 0.135[(0.5Re_\Omega^2 + Re_\infty^2 + Gr)]^{1/3} \tag{3}$$

It is proposed here to extend this heat transfer correlation to mass transfer process by replacing the Prandtl number with the Schmidt number and the Nusselt number with the Sherwood number. The circumferentiel average Sherwood number values were determined in this study, from the local measurements using the following summation: $\overline{Sh} = \frac{1}{2\pi}\sum_{i=1}^{n} Sh_i \Delta\theta_i$ where n is the total number of measurements and $\Delta\theta_i$ denotes the angle increment around the cylinder. Eq. (3) becomes

$$Sh = 0.135[(0.5Re_\Omega^2 + Re_\infty^2)]^{1/3} \tag{4}$$

Eq. (4) will be plotted as a function of the abscissa $(0.5Re_\Omega^2 + Re_\infty^2)Sc$. Fig. 4 shows the comparison of our data with those of Kays and Bjorklund [4]. The present mass transfer results are plotted for the abscissa from 6.3×10^{10} to 3.8×10^{12}. Fig. 4 shows that the experimental mass transfer data agree well within ±16% with Eq. (3), in the range of $(0.5Re_\Omega^2 + Re_\infty^2)Sc$ from 6.3×10^{10} to 1.5×10^{12}. At higher values of the abscissa, the experimental Sherwood number deviates from Eq. (3). This behavior is especially marked when the free stream Reynolds number increases. For this free stream Reynolds number range, the steep rise in mass transfer may be attributed to the turbulence effects, as was mentioned above. Indeed, at a high free stream Reynolds number, a significant increase of the local mass transfer occurs in the upstream moving surface region, due to a laminar-turbulent transition in the boundary layer followed by a separation zone, as was observed on the phase-averaged local mass transfer.

3.3. Heat, mass and momentum transfer analogy for cylinder without crossflow

The analogy between heat and momentum transfer has been used successfully by Kays and Bjorklund [4] to predict heat transfer coefficients from experimentally measured friction coefficients from a circular cylinder rotating in an infinite environment of air. Their analogy calculations can be expressed as a function of a Nusselt

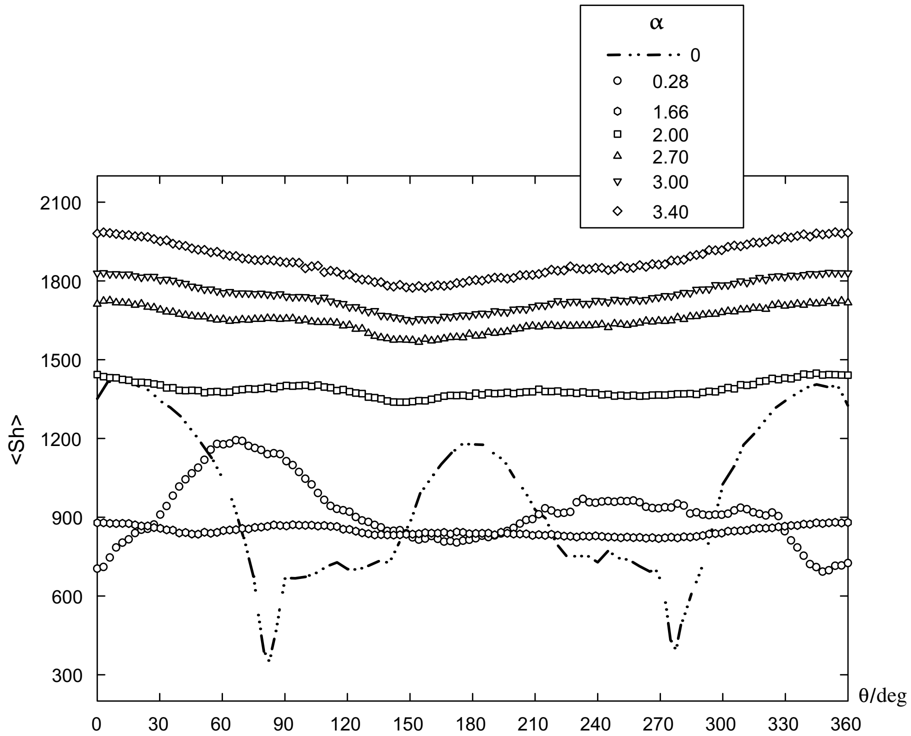

Fig. 3. Phase-averaged mass transfer for $Re_\infty = 17\,000$.

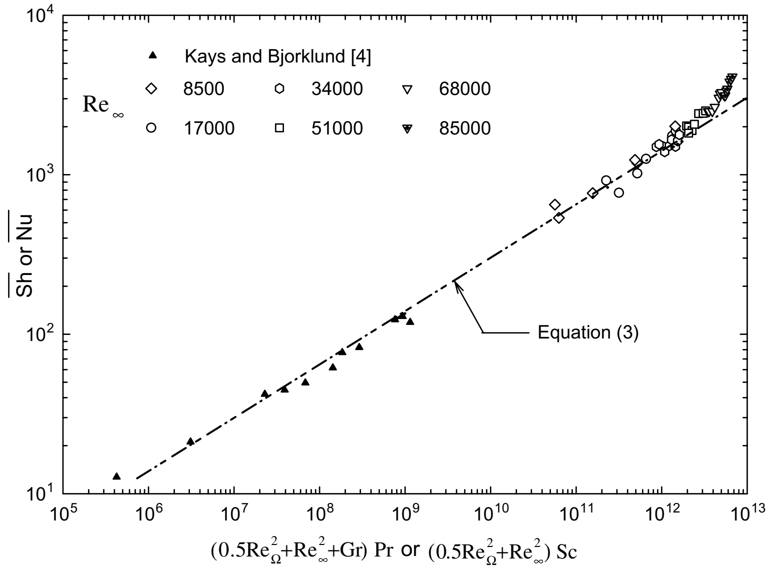

Fig. 4. Average Sherwood and Nusselt numbers as a function of the combined effects of rotation and crossflow.

number, a Reynolds number based on the cylinder peripheral velocity and a friction coefficient C_f. The analogy gives

$$Nu = \frac{Re_\Omega Pr\sqrt{C_f/2}}{(5Pr + 5\ln(3Pr+1) + \frac{1}{\sqrt{C_f/2}} - 12} \qquad (5)$$

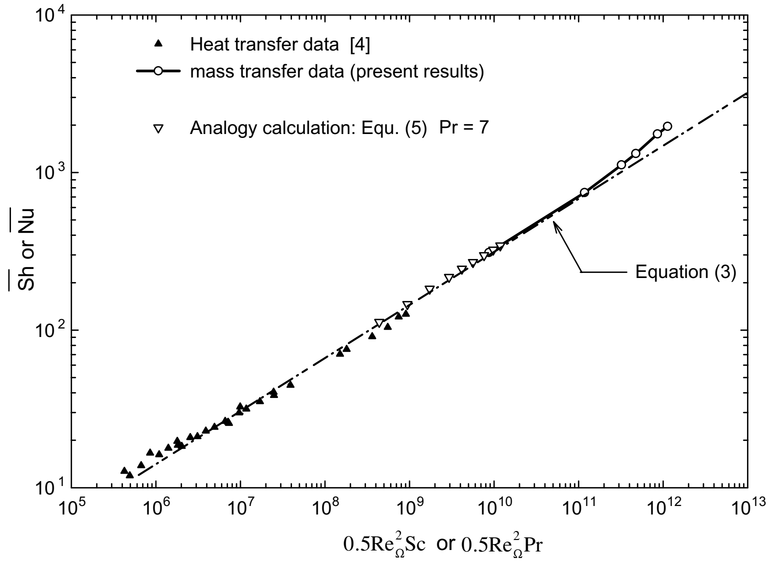

Fig. 5. Average Sherwood and Nusselt numbers as a function of the rotational Reynolds number for a rotating cylinder in a quiescent fluid.

Kays and Bjorklund [4] show that Eq. (5) correlates very well with their experimental data. One of the aims of this study is to extrapolate their results to higher Reynolds numbers and to fluid of a higher Prandtl number ($Pr \approx 7$). Use of Eq. (5) requires knowledge of the friction coefficient. This problem was overcome by using the electrochemical method to determine the local wall shear stress on a rotating cylinder without crossflow. Mass transfer from the rotating cylinder in a quiescent fluid were determined for rotating Reynolds numbers in a range from 1100 to 58 000. The experimental Sherwood numbers are plotted in Fig. 5 as a function of $0.5Re_\Omega^2 Sc$. For the abscissa up to 8×10^9, the experimental mass transfer data are slightly above the curve represented by Eq. (5), with $Re_\infty = 0$. For higher rotating Reynolds numbers, the mass transfer data increase and deviate from the correlation curve proposed by Kays and Bjorklund [4]. This deviation is probably due to the effects of turbulence already observed in the case of a crossflow. Also shown in Fig. 5, are the results of the heat and momentum transfer analogy calculation according to Eq. (5). In the range of the abscissa from 4×10^8 to 1.2×10^{10}, the heat-and-momentum-transfer-analogy solution correlates very well with the experimental mass transfer. This study shows that Eq. (3) proposed by Kays and Bjorklund [4] may be applicable to the mass transfer process for a rotating cylinder with and without crossflow. Moreover, the use of the analogy between heat and momentum transfer, associated to an accurate knowledge of the skin friction, allows the corresponding heat transfer coefficient to be easily predicted.

4. Conclusion

Detailed measurements of the local mass transfer from a rotating cylinder in a crossflow are obtained by using the electrochemical method. The experimental results may be related to the corresponding heat transfer process by means of the analogy between heat and mass transfer. The following conclusions can be drawn:

(a) The local phase-averaged mass transfer analysis showed that the upstream moving surface of the rotating cylinder contribute the most to the mass transfer enhancement, especially for high freestream Reynolds numbers for which a local turbulent flow occurs.
(b) The good correlation between the local wall shear stress and the Sherwood number is a consequence of the strong interaction between the momentum and mass transfer processes.
(c) The combined effect of rotation and crossflow can be correlated by the equation $\overline{Sh} = 0.135[(0.5Re_\Omega^2 + Re_\infty^2)Sc]^{1/3}$. This equation generalizes an equation proposed by some previous authors for the heat transfer process, to a wider range of both rotating and freestream Reynolds numbers. It was shown that for freestream Reynolds numbers above 51 000, this correlation becomes questionable because the flow field state changes drastically.
(d) Heat transfer process can be predicted accurately by heat and momentum transfer analogy for a rotating cylinder in a quiescent fluid. This was made possible

by the local wall shear stress measurements with the electrochemical method.

References

[1] V.T. Morgan, The overall convective heat transfer from smooth circular cylinders, Adv. Heat Transfer 11 (1975) 199–264.

[2] A. Zukauskas, J. Ziugda, Heat Transfer of a Cylinder in Cross Flow, Springer-Verlag, 1985, pp. 97–127.

[3] J.W. Scholten, D.B. Murray, Unsteady heat transfer and velocity of a cylinder in cross flow—I. Low freestream turbulence, Int. J. Heat Mass Transfer 41 (10) (1998) 1139–1148.

[4] W.M. Kays, J.S. Bjorklund, Heat Transfer from a rotating cylinder with and without crossflow, Trans. ASME 80C (1958) 70–78.

[5] H. Peller, V. Lippig, D. Straub, R. Waibel, Thermofluiddynamic experiments with a heated and rotating circular cylinder in cross flow, Part 1: Subcritical heat transfer measurements, Exp. Fluids 2 (1984) 113–120.

[6] H. Peller, Thermofluiddynamic experiments with a heated and rotating circular cylinder in cross flow, Part 2.1: Boundary layer profiles and location of separation points, Exp. Fluids 4 (1986) 223–231.

[7] H. Peller, D. Straub, Thermofluiddynamic experiments with a heated and rotating circular cylinder in cross flow, Part 2.2: Temperature boundary layer profiles, Exp. Fluids 6 (1988) 111–114.

[8] R. Shimada, T. Ohkubo, T. Kobayashi, S. Kumagai, Heat transfer from a rotating cylinder with and without cross flow, Heat Transfer Jpn. Res. 21 (1992) 109–122.

[9] R.J. Goldstein, J. Karni, The effect of a wall boundary layer on local mass transfer from a cylinder in crossflow, Trans. ASME, J. Heat Transfer 106 (1984) 260–267.

[10] L. Labraga, N. Bourabaa, T. Berkah, Wall shear stress from a rotating cylinder in cross flow using the electrochemical technique, Exp. Fluids 33 (2002) 488–496.

[11] M. Lebouché, M. Martin, Convection forcée autour du cylindre; sensibilité aux pulsations de l'écoulement externe, Int. J. Heat Mass Transfer 18 (1975) 1161–1175.